Lidija Ćurković[1], Zrinka Švagelj[1], Krešimir Grilec[1], Gorana Baršić[1], Vilko Mandić[2], Irena Žmak[1], Ivana Gabelica[1]

Comparison of Erosion Rate of Slip Cast Monolithic and Composite Ceramics

[1] Faculty of Mechanical Engineering and Naval Architecture, University of Zagreb, Zagreb, Croatia
[2] Faculty of Chemical Engineering and Technology, University of Zagreb, Zagreb, Croatia

Abstract

In this paper, the solid particle erosion wear of slip cast monolithic alumina (Al_2O_3) and alumina–zirconia (Al_2O_3–ZrO_2) composite ceramics was investigated. Three groups of samples were prepared: (i) monolithic alumina (Al_2O_3); (ii) composite alumina–zirconia (Al_2O_3–ZrO_2) containing 99 wt. % Al_2O_3 and 1 wt. % ZrO_2 and (iii) composite alumina–zirconia (Al_2O_3–ZrO_2) containing 90 wt. % Al_2O_3 and 10 wt. % ZrO_2. X-ray diffraction and scanning electron microscopy (SEM) were used to investigate the phase composition, the crystallite size, and the morphology of the sintered monolithic and composite ceramic samples. The erosive wear behaviour was studied under different impact angles (30°, 60°, 90°) of silicon carbide (SiC) particles as erodent. Erosion mechanisms of all prepared ceramic samples were evaluated by measuring the surface roughness parameters (R_a, R_z, and R_{max}) and the erosion rate. The obtained results showed that the tribological properties of the monolithic Al_2O_3 can be improved with the addition of ZrO_2. It was found that the erosion resistance increases with the increasing amount of ZrO_2 in the composite Al_2O_3–ZrO_2 ceramics. It was found that ZrO_2 grains are homogenously distributed in the alumina matrix, zirconia grain size is smaller than alumina grains, and that the alumina grain size is reduced by the addition of zirconia.

Keywords: *slip casting, erosion rate, monolithic alumina, alumina–zirconia composite ceramics.*

1. Introduction

Ceramic materials are, in general, divided into conventional ceramics and advanced ceramics. The use of conventional ceramics is growing at a slow rate, and some of their branches even show a decreasing tendency, for example refractory materials. In contrast to the conventional ceramics, the market for advanced ceramics is large and continuously growing. The production of advanced ceramics is very important and is one of the branches with highest economic potential in the developed countries and has received a great deal of attention from many fields of the industry. The appropriate forming technology for green bodies is important to manufacture high-quality advanced ceramics. Slip casting is an old forming technique in the ceramic industry and a method for the preparation of homogeneous large green bodies with a complex shape. Conventionally, plaster and resin are used for slip casting moulds. Improvement in slip properties and forming technologies is the way to improve the reliability of advanced ceramics and to lower their cost. Therefore, a lot of effort is put into the development of low-cost technologies for complex ceramic components. The near-net-shape forming of advanced ceramics excite the greatest interest. The following forming processes are currently in the stage of commercialisation or development: pressure slip casting, freeze casting, powder injection moulding, tape casting/lamination, rapid prototyping, and colloidal processing of powders. The technologies based on the colloidal processing, such as slip casting, gel casting, electrophoretic casting, hydrolysis-assisted solidification, direct coagulation casting, etc. are of great interest due to their ability to reduce the critical defects which can occur during the manufacturing process [1-8].

Slip casting is the most adequate technology to produce complex ceramic components. It is a simple, reliable, flexible, cost-effective, and pollution-free procedure, but it requires an adequate understanding of colloid suspensions and their behaviour. This knowledge is crucial for the optimization of technologies to produce improved ceramic products, e.g., slip, gel, and centrifugal casting, injection moulding, and coating. The properties of ceramic products strongly depend on the size of ceramic powder particles: when particles are smaller, the sintering is better and, consequently, product properties are better, too. On the other hand, ceramic particles smaller than 1μm, in combination with high suspension concentration, increase the suspension viscosity. The increased suspension viscosity is a consequence of greater interaction among particles, which can lead to agglomeration or flocculation [1-8]. This particle interaction can be controlled with additives (dispersants). For a multi-component system, the selection of the

dispersants becomes more critical because it might be difficult to find a dispersant that is optimal for all used components (Figure 1).

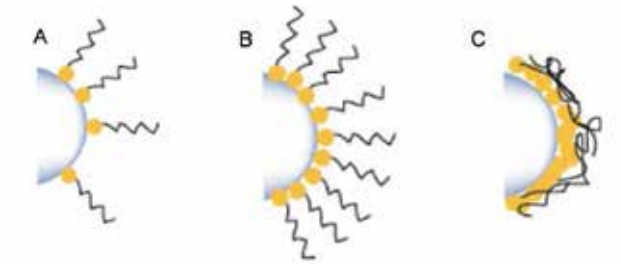

Fig. 1. Amount of additive: (A) too little, (B) optimal, (C) too much.

The particle interaction can be controlled with chemical additives in three different ways: electrostatic, steric, and electrosteric (a combination of the first two). The influence of additives (different dispersants) on the ceramic suspension stability has been extensively researched [1-8]. Despite that, the worldwide ceramic industry requires new, better additives to improve the slip casting process and, consequently, the ceramic products.

The slip casting process can be used for the manufacturing of monolithic and composite ceramic products of different sizes and shapes with homogeneous microstructure. In the past decade, several studies on rheological properties of binary systems, such as Al_2O_3–ZrO_2 composites, were performed [9-14]. For a multi-component system, the appropriate dispersant selection becomes more critical because it might be difficult to find a dispersant that is optimal for all used components. Slip casting of advanced ceramics based on alumina–zirconia requires the use of a dispersant, a binder, and an agent to prevent excessive grain growth. There are many commercially available dispersants and binders that can be used for the advanced ceramics slip casting process. However, the determination of a suitable combination and the quantification of optimal additions of the dispersant/binder pair with the starting particle size at the nano- and micro-levels can be time-consuming.

The suspension stability must be well achieved to establish complete control over suspension rheological properties. The sedimentation tests, the measurement of the zeta-potential and the apparent viscosity measurements are often used for the suspension stability estimation [3,10].

Aluminium oxide (Al_2O_3) or alumina, is an exceptionally important ceramic material and one of the most widely used advanced ceramics, which has many technological applications [2-4,15-18]. It has some extraordinary properties, like high hardness, chemical inertness, wear resistance and a high melting point. Because of their excellent properties, alumina ceramics are widely used for many refractory materials, grinding media, cutting tools and high temperature bearings. Therefore, a variety of mechanical parts and critical components used in chemical process environments, where materials are subjected to aggressive chemical atmosphere, extremely high temperatures and pressures, are typically made of alumina. Over the past thirteen years, several papers on corrosion [15,16,19,20], mechanical [10,17,21-24] and tribological [18,25-31] properties of advanced ceramics have been published. Industrial interest has been aroused as well, considering the broad array of advanced ceramic products for different applications, especially for tribological and corrosion applications.

Alumina ceramics (Al_2O_3) has the following properties: low fracture toughness (<5 MPa·m$^{1/2}$), low bending strength (<600 MPa) and high wear resistance. On the other side, yttria-stabilized tetragonal zirconia (t-ZrO_2) has high fracture toughness (6 MPa·m$^{1/2}$ to 15 MPa·m$^{1/2}$), high bending strength (1000 MPa to 1500 MPa) and high wear resistance. Mechanical and tribological properties of alumina can be improved by the addition of t-ZrO_2 (yttrium-stabilized tetragonal zirconia, Y-TZP). A disadvantage of pure zirconia is its low thermal conductivity compared to alumina: alumina has a thermal conductivity that is at least 3 times higher than that of zirconia. In a tribological contact, frictional heating occurs, and the low thermal conductivity of zirconia may cause thermally induced crack formation, followed by severe wear processes [10]. Improved properties of the monolithic alumina ceramics can be obtained by the incorporation of a small amount of zirconia (ZrO_2) particles in the alumina ceramic matrix to produce advanced Al_2O_3–ZrO_2 composite ceramics [10-14,30] (Figure 2).

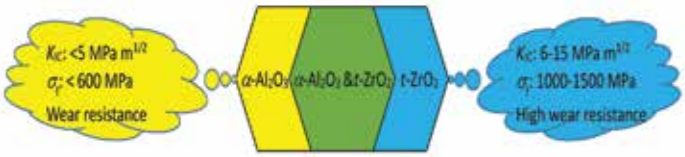

Fig. 2. Improved properties of alumina ceramics by addition of t-ZrO_2.

Erosion wear due to the flow of solid–liquid mixtures has shown dependence on many interrelated parameters: the properties of the target material, the present erodents and the carrier liquid are the major parameters affecting the material removal rate under similar flow conditions [32]. Solid particle erosion is the loss of material that results from repeated impacts of small, solid particles. In some cases, it is a useful phenomenon, as in sandblasting and high-speed abrasive waterjet cutting, but usually it is a serious problem in many engineering systems, including steam and jet turbines, pipelines and valves carrying particulate matter, and fluidized bed combustion systems. Solid particle erosion can occur in

a gaseous or liquid medium containing solid particles [33]. Erosive wear occurs by plastic deformation and/or brittle fracture, depending on the material being eroded and on the operating parameters. Ductile materials will wear by undergoing the process of plastic deformation, in which the material is removed by displacing or cutting by the eroding particles. In brittle materials, on the other hand, the material will be removed by the formation and intersection of cracks that radiate from the impact point of the eroding particles [34]. Ductile materials, such as pure metals, have the highest erosion rate at low angles of incidence (typically 15º to 30º), while for brittle materials the highest impact erosion rate usually occurs at 90º [33].

In this investigation, solid particle erosion tests were conducted to investigate the erosion wear behaviour of the slip cast monolithic high purity alumina and alumina–zirconia composite ceramics at different erodent particles impact angles at the room temperature. The erodent impact angles were 30°, 60° and 90°. Dry silicon carbide (SiC) was used as an erodent. Erosion mechanisms of all prepared ceramic samples were evaluated by measuring the erosion rate and roughness parameters (R_a, R_z, R_m).

2. Materials and methods

2.1. Preparation of green bodies of monolithic and composite ceramics by slip casting.

The green bodies of monolithic alumina (Al_2O_3) and alumina–zirconia (Al_2O_3–ZrO_2) composite ceramics were obtained by slip casting method. The first step in slip casting is the preparation of stable highly concentrated aqueous suspensions (the so-called "slips").

All suspensions contained 70 wt. % of dry ceramic powder and 30 wt. % of deionized water. The following components were used for the preparation of highly concentrated aqueous suspensions:

- high-purity α-Al_2O_3, with the average particle size of 300–400 nm (Alcan Chemicals, Stamford, CT, USA);
- high-purity t-ZrO_2 stabilized with 3 mol % of yttria (Y_2O_3), with the average particle size of 25 nm (SkySpring Nanomaterials Inc., Houston, TX, USA);
- an alkali-free anionic polyelectrolyte dispersant Dolapix CE 64 (Zschimmer & Schwarz GmbH & Co KG Chemische Fabriken, Lahnstein, Germany), with the molecule structure shown in Figure 3;
- 70 wt. % aqueous solution of the ammonium salt of polymethacrylic acid (PMAA–NH4);
- magnesium oxide added as magnesium aluminate spinel ($MgAl_2O_4$) made by Alfa Aesar, Haverhill, MA, USA, used to inhibit the abnormal alumina grain growth during the sintering process;
- deionized water.

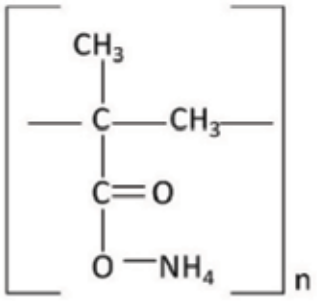

Fig. 3. The molecule structure of dispersant Dolapix CE 64.

Three groups of 70 wt. % alumina–zirconia aqueous suspensions (slips) were prepared:

- monolithic Al_2O_3 (composition: 100 wt. % Al_2O_3–0 wt. % ZrO_2);
- composite Al_2O_3–ZrO_2 ceramics (composition: 99 wt. % Al_2O_3–1 wt. % ZrO_2);
- composite Al_2O_3–ZrO_2 ceramics (composition: 90 wt. % Al_2O_3–10 wt. % ZrO_2).

The dispersant and the ceramic powders were added into the distilled water to form suspensions. They were homogenized for 90 min, at 300 rpm in the planetary ball mill (PM 100, Retsch GmbH, Germany). The grinding jar and balls used for homogenization were made of alumina as well to avoid sample contamination. Prior to the apparent viscosity measurement and forming of the green bodies, suspensions were ultrasonically treated in the ultrasonic bath BRANSONIC 220 (Branson Ultrasonics Corp., Danbury, CT, USA) with 50 kHz and 120 W to remove any trapped air bubbles and break down agglomerates.

The prepared suspensions were subjected to the rheological measurements on the rotational viscometer DV-III Ultra (Brookfield Engineering Laboratories, Inc., MA, USA) with a small sample chamber and spindle SC4-18. Samples were tempered at 25 °C ± 1 °C with the assistance of thermostatic bath Lauda Eco RE 415 (LAUDA-Brinkmann, LP, USA). Viscosity was determined at the shear rate of 50 s^{-1}, which is the exact shear rate of gravity slip casting.

2.2. Sintering of monolithic alumina and composite alumina–zirconia ceramics

Green bodies of monolithic Al_2O_3 and composite Al_2O_3–ZrO_2 ceramics were formed by the slip casting forming

method. After measuring the apparent viscosity, the suspensions with the minimum apparent viscosity were poured into previously prepared gypsum moulds and air-dried. The gypsum mould draws water from the poured slip and gives a form to the green body.

The prepared green bodies of monolithic Al_2O_3 and composite Al_2O_3–ZrO_2 ceramics were sintered by the conventional sintering in an electric kiln at 1650 °C, according to the sintering regime shown in Figure 4.

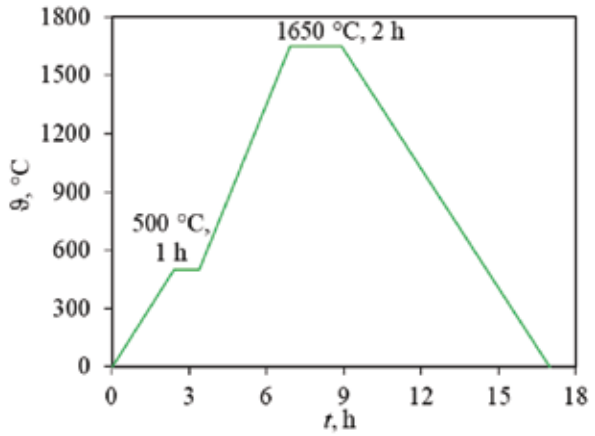

Fig. 4. Sintering regime of monolithic Al_2O and Al_2O_3–ZrO_2 composite ceramics.

Sintered samples (dimensions of 17 mm × 17 mm × 17 mm) of monolithic alumina and zirconia–alumina (with the addition of 1 and 10 wt. % ZrO_2) composite ceramics were prepared for the erosion tests by grinding and polishing, as per the standard ceramographic technique [35], to have a smooth surface finish. After polishing, the specimens were thoroughly ultrasonically cleaned in pure 94 vol. % alcohol and dried in a sterilizer at 150 ºC ± 5 ºC for 4 hours. The specimens were then annealed at 1200 °C for 360 min to eliminate any residual stresses that may have occurred during grinding and polishing.

2.3. Characterisation of monolithic and composite ceramics

Powder X-ray diffraction analysis (XRD) was used to investigate phase composition and crystallite size of monolithic and composite samples. XRD analysis was performed on XRD-6000 (Shimadzu, Tokyo, Japan) using CuKα radiation at an accelerating voltage of 40 kV and a current of 30 mA. All samples were analysed in a 2θ range of 5° to 75° in a continuous mode with a 0.02° 2θ step and a scan rate of 0.6 s.

The surface morphology of the sintered ceramic samples was determined by the scanning electron microscope (SEM), Tescan Vega Easy Probe 3, operating at 10 kV equipped with secondary (SE) and backscattered electron (BSE) detectors (Tescan, Brno, Czech Republic).

2.4. Erosion wear rate testing

The erosion test was carried out using an erosion testing apparatus (Figure 5), where samples were subjected to erosive wear of dry silicon carbide (SiC) particles as erodent.

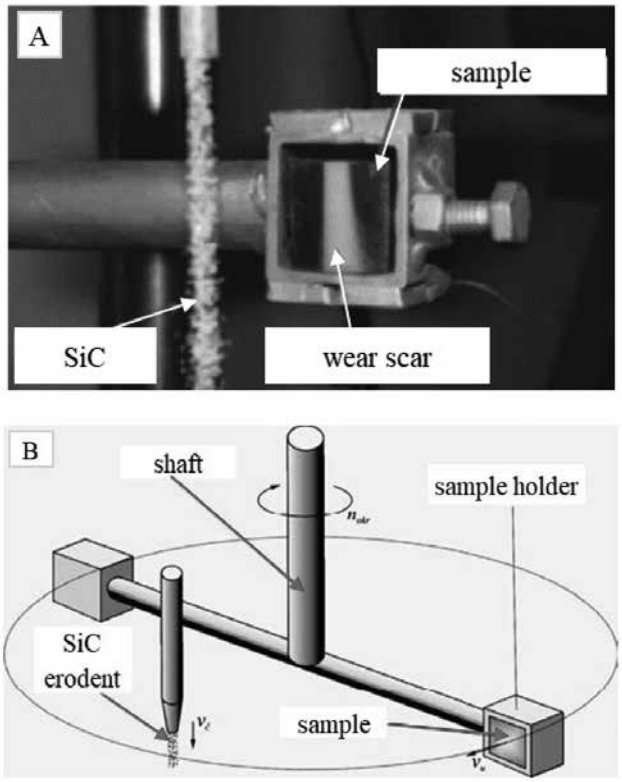

Fig. 5. (A) Sample holder in erosion test equipment, (B) scheme of sand equipment for erosion testing [18,25].

The erodent impact angles were 30°, 60° and 90°. When placed in the sample holders, the samples were span at about 1440 rpm through the seeping beam of the erodent powder. Two samples were eroded at the same time, one in each sample holder. The erodent powder was taken away by means of gravity and stored. Each test took 13 minutes and 53 seconds, to achieve approximately 20 000 impacts per sample and was carried out at room temperature. The erosion tests were repeated five times for each sample and each impact angle.

The abrasive particles properties are presented in Table 1 and the SEM micrograph of the used SiC erodent is shown in Figure 6. The SiC particles were sharp and angular, as seen in Figure 6.

Table 1. Properties of erodent particles: hardness (HV), density (ρ, kg/m^3), fracture toughness (K_{IC}, MPa·m$^{1/2}$).

Erodent	Average particle size, μm	HV	ρ, kg/m^3	K_{IC}, MPa·m$^{1/2}$
SiC	350	2800	3300	3.52

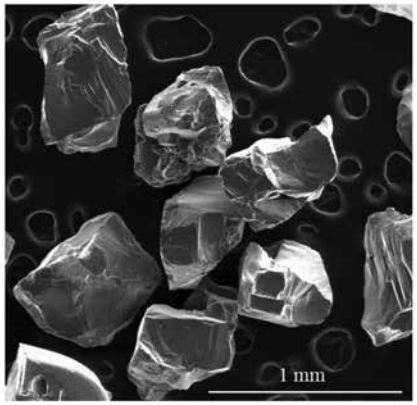

Fig. 6. SEM micrograph of erodent SiC particles.

The erosion mechanisms of all prepared ceramic samples were evaluated by measuring the following parameters before and after erosion:

- the surface roughness parameters (R_a, R_z, and R_{max});
- the erosion rates.

More precise information on erosion resistance was obtained by measuring the roughness parameters of the eroded surfaces. The roughness of each specimen was measured on five different tracing lanes using Perthometer S&P 4.5 (Feinprut Perthen GmbH, Göttingen, Germany). Before and after the erosion experiments, cleaned and dried samples of alumina ceramics were weighed in an electronic analytical balance to an accuracy of ± 0.01 mg. The amount of wear was determined by measuring the weight loss of ceramic samples (Δm).:

$$\Delta m = m_i - m_f \quad (1)$$

where m_i and m_f are the mass of the target material before and after the impact, respectively. The erosion rate is calculated using the weight loss approach [36]:

$$E = \frac{\Delta m}{m_e} = \frac{m_i - m_f}{m_e} \quad (2)$$

where E is the erosion rate (Δg/g), and me is the mass of the erodent.

3. Results and discussion

3.1. Apparent viscosity measurements

Apparent viscosity measurements were used for the suspension stability estimation. The suspension viscosity is at a minimum value when the dispersion of the ceramic particles is optimal. The rheological measurements showed that the measured apparent viscosity increases with the increasing zirconia content (Figure 7 and Table). The optimal amount of the dispersant Dolapix CE 64 also increases with the increasing zirconia content. The diagram in Figure 7 shows the apparent viscosity at a shear rate of app. 50 s^{-1}, which is the shear rate of the gravity slip casting.

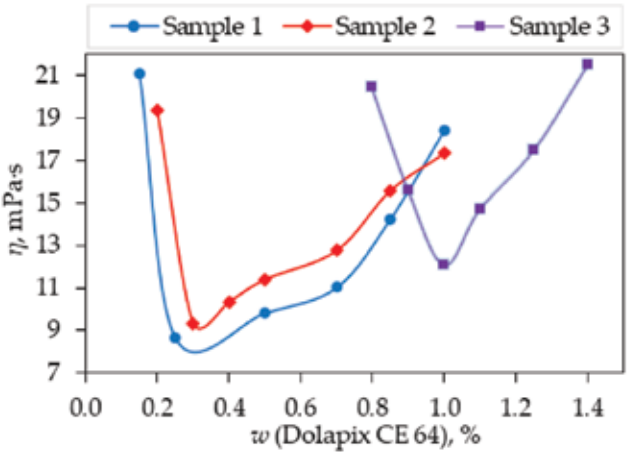

Fig. 7. Dependence of apparent viscosity on applied amount of Dolapix CE 64.

The compositions of all suspensions with the optimal amount of Dolapix CE 64 and the magnesium aluminate spinel are listed in Table 2.

Table 2. Compositions and apparent viscosity of 70 wt. % suspensions for slip casting of monolithic Al_2O_3 and Al_2O_3–ZrO_2 composite ceramics.

Suspension sample	**1**	**2**	**3**
wt. (Al_2O_3+ZrO_2), %	70	70	70
wt. (H_2O), %	30	30	30
wt. (Al_2O_3 in powder mixture), %	100	99	90
wt. (ZrO_2 in powder mixture), %	0	1	10
*wt.** (DOLAPIX CE 64), %	0.25	0.30	1.00
η, mPa·s	8.67	9.35	12.08

**wt.*, weight percent based on the dry ceramic powder

The optimal amounts of the dispersant and the magnesium aluminate spinel for each suspension were determined in previous research [10].

From the diffractogram in Figure 8, the qualitative phase composition was determined for all samples. The diffractogram indicates that the hexagonal Al_2O_3 consists of only α-Al_2O_3 crystalline phase (corundum) (ICDD PDF#46-1212). Qualitatively, sintered zirconia-toughened alumina composite shows the presence of α-Al_2O_3 (ICDD PDF#46-1212) as the main phase, t-ZrO_2 (ICDD PDF#42-1164) as the minor phase and m-ZrO_2 (ICDD PDF#37-1484) in traces. With an increase in the zirconia content, both t-ZrO_2 and m-ZrO_2 intensity

increased (the intensity increase of the t-ZrO_2 phase peak is highlighted).

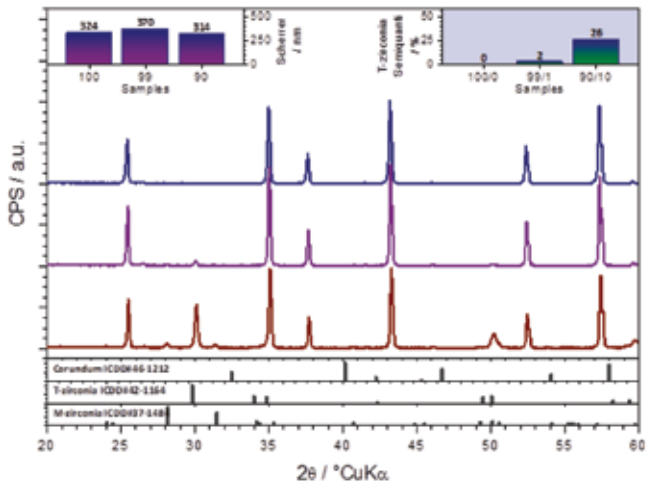

Fig. 8. Powder X-ray diffraction (XRD) results of monolithic Al_2O_3 (100 wt. % Al_2O_3), and Al_2O_3–ZrO_2 composite ceramics (1 wt. % ZrO_2 + 99 wt. % Al_2O_3 and 10 wt. % ZrO_2 +90 wt. % Al_2O_3).

The intensity of the t-ZrO_2 strongest peak and m-ZrO_2 strongest peak was compared to allow an insight into the mutual dependence of the zirconia phases (t-ZrO_2 to m-ZrO_2 ratio) as a function of the zirconia loading. With the introduction of 1 wt. % of zirconia, the relative content of the m-ZrO_2 was about 15 wt. % (i.e., 85 wt. % t-ZrO_2). However, the calculation of the ratio of zirconia phases that are present in total of about 1 wt. % in the analysed material may be questionable. Upon an increase in the zirconia loading to 10 wt. %, the relative presence of the m-ZrO_2 was reduced to about 7 wt. % (93 wt. % t-ZrO_2). As the microstructure is considered, the use of monolithic α-alumina yields crystallites of about 324 nm in size. Crystallite size was calculated by applying the Scherrer equation on the XRD patterns. Alumina crystallite size was increased to 370 nm by the addition 1 wt. % of zirconia to ceramic composites. The addition of 10 wt. % of zirconia to the composite reduced the crystallite size of alumina to 314 nm, thus favourably impacting the microstructure.

The results of the SEM analysis of the fracture surface of the sintered monolithic Al_2O_3 and Al_2O_3–ZrO_2 composite ceramics are shown in Figure 9. The ZrO_2 particles (the brighter phase) are distributed in the Al_2O_3 matrix, with some agglomerates of ZrO_2 and some pores.

The erosive wear behaviour of monolithic alumina and alumina–zirconia composite ceramics samples were evaluated by measuring:

- the roughness parameters (R_a, R_z, and R_{max});
- the erosion rate.

All measurements were made before and after the surface erosion of the investigated samples. SiC particles were used as erodent at impact angles of 30°, 60° and 90°.

The sintered samples were subjected to the solid particle erosion to determine whether the addition of the zirconia nanoparticles improves the erosion resistance of alumina. Solid particle erosion can be defined as a degradation of the material caused by repeated impacts of small solid particles [18,25,33,37]. According to the literature, the lower impact angle (30°) corresponds to the abrasive erosion, while the higher impact angle (90°) correlates with the impact erosion [18,25,33,37]. Wear mechanisms were analysed by comparing the surface roughness (microroughness) parameters before and after the erosion test using a profilometer. It is assumed that higher surface roughness after the test indicates lower erosion resistance [18,25].

Three main roughness parameters were obtained from this test:

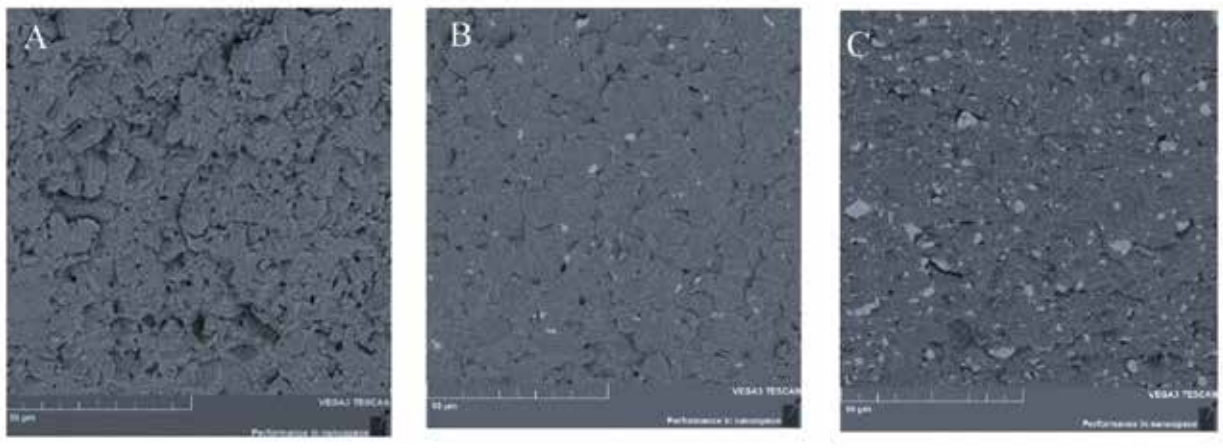

Fig. 9. SEM micrographs of fracture surface morphology of Al_2O_3–ZrO_2 composite ceramics with different ZrO_2 content: (A) 0 wt. %, (B) 1 wt. %, (C) 10 wt. %, prepared by slip casting and sintered at 1650 °C.

- R_a - the roughness average;

- R_z - the ten-point average of the profile;

- R_{max} - the maximum between the peak and the valley.

In Figure 10 the obtained values of the roughness parameters before and after erosion with SiC particles at 30°, 60° and 90° impact angles are presented. The roughness parameters (R_a, R_z, and R_{max}) are presented as mean values of five measurements and standard deviation ($\bar{x} \pm 2\,s$).

After the erosion test, all surface roughness parameters increased for all samples. The obtained results confirmed that these types of slip cast monolithic and composite ceramics are more sensitive to impact than to abrasive erosion, since all surface roughness parameters were higher for the higher impact angle (90°) for all samples, Figure 10.

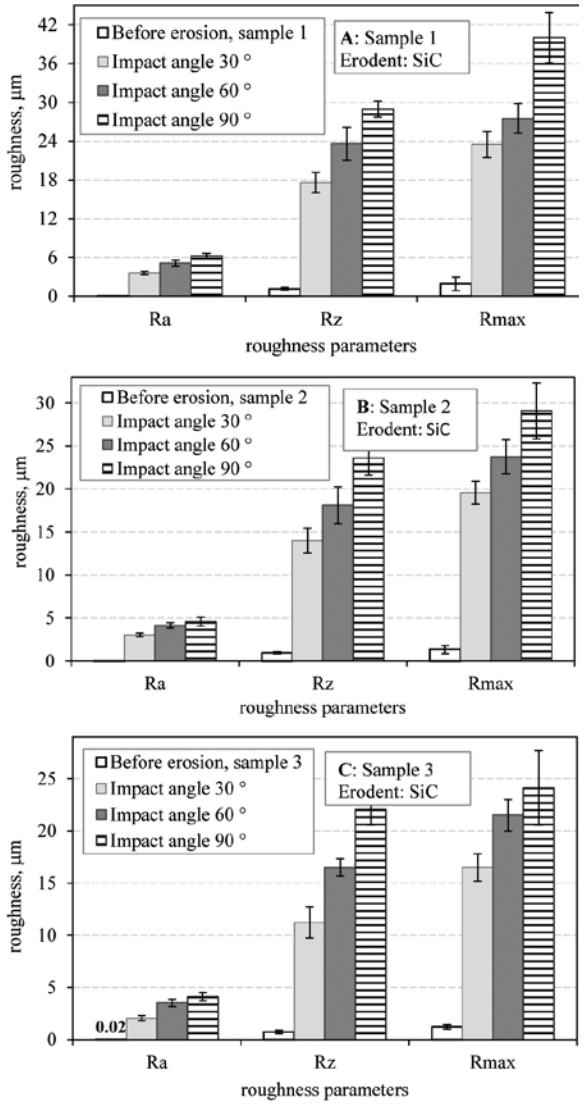

Fig. 10. Values of roughness parameters ($\bar{x} \pm 2\,s$) before and after erosion with SiC particles at 30°, 60° and 90° impact angles for (A) sample 1: 100 wt. % Al_2O_3, (B) sample 2: 99 wt. % Al_2O_3+1 wt. % ZrO_2, (C) sample 3: 90 wt. % Al_2O_3+10 wt. % ZrO_2.

This investigation also confirmed the hypothesis that the tribological properties of the alumina can be improved with the addition of zirconia nanoparticles: all surface roughness parameters were higher for the monolithic alumina than for the alumina–zirconia composites at all impact angles.

Figure 11 illustrates the erosion rates (mean value and standard deviation, $\bar{x} \pm 2\,s$) of alumina ceramics plotted against the impact angle. The erosion rate is determined according to equation 2. Tests were repeated five times for each experimental condition. The erosion wear tests for all ceramic samples were performed by SiC particles at impact angles of 30°, 60° and 90°. The obtained results indicate that both composite ceramics were more resistant to the impact erosion than monolithic alumina ceramics.

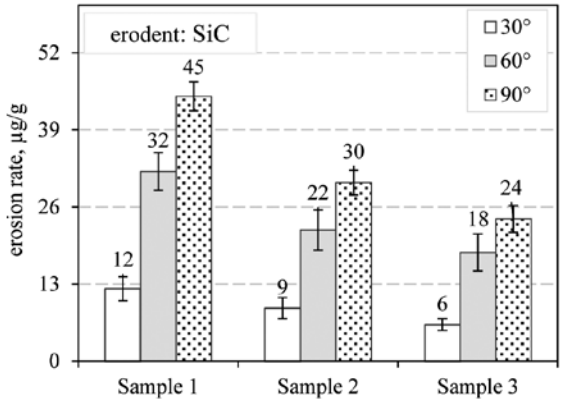

Fig. 11. Erosion rate ($\bar{x} \pm 2\,s$) after erosion with SiC particles at 30°, 60° and 90° impact angles for:
sample 1 (100 wt. % Al_2O_3),
sample 2 (99 wt. % Al_2O_3+1 wt. % ZrO_2) and
sample 3 (90 wt. % Al_2O_3+10 wt. % ZrO_2).

From the results presented in Figure 11 it is obvious that the erosion rates of all ceramic samples increase with increasing impact angle, with the maximum erosion rate occurring at an impact angle of 90°. Since the lower impact angle (30°) is related to the abrasive type of erosion, and the higher impact angle (90°) is related to the impact erosion, it can be concluded that all studied ceramic samples are more resistant to abrasive than to impact erosion.

4. Conclusions

The green bodies of the monolithic Al_2O_3 and composite Al_2O_3–ZrO_2 ceramics (composition: 99 wt. % Al_2O_3 + 1 wt. % ZrO_2, and 90 wt. % Al_2O_3 and 10 wt. % ZrO_2) were formed by the slip casting process in a plaster mould. After drying and green machining, green bodies were sintered at a temperature of 1600 °C.

SEM analysis of the prepared composite ceramics showed that the ZrO_2 particles are well dispersed in

Al_2O_3 matrix for both samples (containing 1 wt. % and 10 wt. % of ZrO_2), with some agglomerates of ZrO_2 and some pores. The relative presence of the m-ZrO_2 was found to be about 7 wt. % vs. 93 wt. % of t-ZrO_2 (for the sample with 10 wt. % ZrO_2).

Alumina crystallite size increased from 324 nm to 370 nm by the addition 1 wt. % of ZrO_2 to the ceramic composite. Conversely, the addition of 10 wt. % of ZrO_2 reduced the Al_2O_3 crystallite size to 314 nm.

The sintered samples were subjected to the erosion resistance test using the SiC particles under different impact angles (30°, 60°, 90°) and the following conclusions were drawn:

- Surface roughness parameters increased after erosion.
- All surface roughness parameters were higher for monolithic alumina than for zirconia–alumina composite ceramics.
- The erosion rate decreased with the increase of the ZrO_2 content in the alumina matrix.
- All ceramic samples were more sensitive to impact than to abrasive erosion.

Acknowledgements

This work has been fully supported by the Croatian Science Foundation under the project IP-2016-06-6000: “Monolithic and composite advanced ceramics for wear and corrosion protection” (WECOR).

References

[1] Wu, L., Huang, Y., Liu, L. Meng, Interaction and stabilization of DMF-based alumina suspensions with citric acid. Powder Technol, 203, 477–481 (2010).

[2] Vukšić, M., Žmak, I., Ćurković, L., Ćorić, D., Effect of Additives on Stability of Alumina—Waste Alumina Suspension for Slip Casting: Optimization Using Box-Behnken Design. Materials, 12, 1–16 (2019).

[3] Sever, I., Žmak, I., Ćurković, L., Švagelj, Z., Stabilization of highly concentrated alumina suspensions with different dispersants. Transactions of FAMENA, 3(72), 61–70 (2018).

[4] Landek, D., Ćurković, L., Gabelica, I, Kerolli Mustafa, M., Žmak, I., Optimization of Sintering Process of Alumina Ceramics Using Response Surface Methodology. Sustainability, 13, 6739 (2021).

[5] Mohanty, S., Das, B., Dhara, S., Poly(maleic acid) - A novel dispersant for aqueous alumina slurry. J Asian Ceram Soc, 1(2), 184–190 (2013).

[6] Majić Renjo, M., Lalić, M., Ćurković, L., Matijašić, G., Rheological properties of aqueous alumina suspensions. Mater Werkst, 43, 979–983 (2012).

[7] Tallon, C., Limacher, M., Franks, G.V., Effect of particle size on the shaping of ceramics by slip casting. J Eur Ceram Soc, 30, 2819–2826 (2010).

[8] Xu, Y., Mao, X., Fan, J., Li, X., Feng, M., Jiang, B., Lei, F., Zhang, L., Fabrication of transparent yttria ceramics by alcoholic slip-casting. Ceram Int, 43(12), 8839–8844 (2017).

[9] León-Carriedo, M., Gutiérrez-Chavarría, C.A., Rodríguez-Galicia, J.L., Multilayered Zircon-Alumina Components Fabricated by Slip Casting. Materials Science Forum, 755, 145–151 (2013).

[10] Žmak, I., Ćorić, D., Mandić, V., Ćurković, L., Hardness and Indentation Fracture Toughness of Slip Cast Alumina and Alumina-Zirconia Ceramics. Materials, 13, 1–17 (2020).

[11] Guimaraes, F.F.A.T., Silva, K.L., Trombini, V., Pierri, J.J., Rodrigues, J.A., Tomasi, R., Pallone, E.M.J.A., Correlation between microstructure and mechanical properties of Al_2O_3/ZrO_2 nanocomposites. Ceram Int, 35(2), 741–745(2009).

[12] Wakily, H., Mehrali, M., Metselaar, H.S.C., Preparation of Homogeneous Dense Composite of Zirconia and Alumina (ZTA) using Colloidal Filtration. World Academy of Science, Engineering and Technology, 46, 140–145 (2010).

[13] Sun, L., Sneller, A., Kwon, P., Fabrication of alumina/zirconia functionally graded material: From optimization of processing parameters to phenomenological constitutive models. Materials Science and Engineering A, 488, 31–38 (2008).

[14] Zhang, Y., Sun, M.J., Zhang, D., Designing functionally graded materials with superior load-bearing properties. Acta Biomaterialia, 8, 1101–1108 (2012).

[15] Ćurković, L., Fudurić Jelača, M., Kurajica, S., Corrosion behaviour of alumina ceramics in aqueous HCl and H_2SO_4 solutions. Corros Sci, 50, 872–878 (2008).

[16] Ćurković, L., Fudurić Jelača M., Dissolution of alumina ceramics in HCl aqueous solution. Ceram Int, 35, 2041–2045 (2009).

[17] Ćurković, L., Lalić, M., Šolić, S., Analysis of the indentation size effect on the hardness of alumina ceramics using different models. Kovove Materialy-Metallic Materials, 47, 89–93(2009).

[18] Ćurković, L., Kumić, I., Grilec, K., Solid particle erosion behaviour of high purity alumina ceramics. Ceram Inter, 57, 29–35(2011).

[19] Kurajica, S., Mandić, V., Ćurković, L., Mullite ceramics acid corrosion kinetics as a function of gel homogeneity, Biointerface Research in Applied Chemistry, 7(6), 2295–2299 (2017).

[20] Živko-Babić, J., Lisjak, D., Ćurković, L., Jakovac, M., Estimation of chemical resistance of dental ceramics by neural network. Dent Mater, 24, 18–27 (2008).

[21] Majić, M., Ćurković, L., Ćorić, D., Load dependence of the apparent Knoop hardness of SiC ceramics in a wide range of loads. Mater Werkst, 42, 234–238 (2011).

[22] Elsaka, S.E., Elnaghy, A.M., Mechanical properties of zirconia reinforced lithium silicate glass-ceramic. Dent Mater, 32, 908–914 (2016).

[23] Wan, W., Yang, J., Feng, Y., Bu, W., Qiu, T., Effect of trace alumina on mechanical, dielectric, and ablation properties of fused silica ceramics. J Alloys Compd, 675, 64–72 (2016).

[24] Bhattacharya, S., Kundu, R., Bhattacharya, K., Poddar, A., Roy, D., Micromechanical hardness study and the effect of reverse indentation size on heat-treated silver doped zinc-molybdate glass nanocomposites. J Alloys Compd, 770, 136–142 (2019).

[25] Grilec, K., Ćurković, L., Kumić, I., Baršić, G., Erosion mechanisms of aluminium nitride ceramics at different impact angles. Mater Werkst, 42, 712–717(2011).

[26] Celotta, D.W., Qureshi, U.A., Stepanov, E.V., Goulet, D.P., Hunter, J., Buckberry, C.H., Hill, R., Sherikar, S.V., Moshrefi-Torbati, M., Wood, R.J.K., Send erosion testing of novel composites and hard ceramics. Wear, 263, 278–283 (2007).

[27] Wu, T., Zhou, J., Wu, B., Xiong, Y., Effect of Y_2O_3 additives on the wet abrasion resistance of an alumina-based grinding medium. Wear, 356–357, 9–16 (2016).

[28] Wu, T., Zhou, J., Wu, B., Li, W., Effect of La_2O_3 content on wear resistance of alumina ceramics. Journal of Rare Earths, 34, 288–294 (2016).

[29] Pereira de Oliveira, R., Santos, E. dos, Cousseau, T., Sinatora, A., Effect of pH on wear and friction of silicon nitride sliding against alumina in water. Tribol Int, 90, 356–361(2015).

[30] Pulgarin, H.L.C., Garrido, L.B., Albano, M.P., Comparison of different zirconia powders for slip casting of alumina–zirconia ceramics. Advances in Applied Ceramics, 12, 39–45 (2013).

[31] Milak P.C., Minatto F.D., De Noni Jr. A., Montedo O.R.K., Wear performance of alumina-based ceramics - a review of the influence of microstructure on erosive wear. Ceramica, 61, 88–103 (2015).

[32] Desale G.R, Gandhi B.K., Jain S.C., Effect of erodent properties on erosion wear of ductile type materials. Wear, 261, 914–921 (2006).

[33] SM SM Handbook, Friction, lubrication, and wear technology, ASM International, USA, (1992).

[34] Bhushan B., Introduction to Tribology, John Wiley and Sons, USA, (2002).

[35] Chinn, R.E., Ceramography: Preparation and Analysis of Ceramic Microstructures, ASM International, USA, (2002).

[36] Ragav P. Panakarajupally, R.P., Mirza, F., Rassi, J.E., Morscher, G.N., Abdi, F., Choi, S., Solid particle erosion behavior of melt-infiltrated SiC/SiC ceramic matrix composites (CMCs) in a simulated turbine engine environment. Composites Part B, 216, 108860 (2021).

[37] Bhushan B., Introduction to Tribology, John Wiley and Sons, USA. (2002).

Vol. 16(2) 2021 – ISSN 1331-7210

Engineering Power – *Bulletin of the Croatian Academy of Engineering*

Publisher: Croatian Academy of Engineering (HATZ), 28 Kačić Street, P.O. Box 14, HR-10001 Zagreb, Republic of Croatia

Editor-in-Chief: Prof. Vladimir Andročec, Ph.D., President of the Academy retired Full Professor with tenure, University of Zagreb, Faculty of Civil Engineering

Editor: Prof. Zdravko Terze, Ph.D., Vice-President of the Academy University of Zagreb, Faculty of Mechanical Engineering and Naval Architecture

Guest-Editor: Prof. Lidija Ćurković, Ph.D., University of Zagreb, Faculty of Mechanical Engineering and Naval Architecture

Editorial Board: Prof. Vladimir Andročec, Ph.D., Prof. Zdravko Terze, Ph.D., Prof. Vladimir Mrša, Ph.D.

Editorial Board Address: Croatian Academy of Engineering (HATZ), "Engineering Power" – Bulletin of the Croatian Academy of Engineering, Editorial Board, 28 Kačić Street, P.O. Box 14, HR-10001 Zagreb, Republic of Croatia

E-mail: hatz@hatz.hr

Graphical and Technical Editor: Minerva Graphica, Ltd., Zagreb

Proof-reader: Miroslav Horvatić, MA

Press: Tiskara Zelina, Ltd., Zelina

Circulation: 200